Intertwining Topological Order and Broken Symmetry in a Theory of Fluctuating Spin-Density Waves

Shubhayu Chatterjee,[1] Subir Sachdev,[1,2] and Mathias S. Scheurer[1]
[1]Department of Physics, Harvard University, Cambridge, Massachusetts 02138, USA
[2]Perimeter Institute for Theoretical Physics, Waterloo, Ontario, Canada N2L 2Y5
(Received 19 May 2017; revised manuscript received 25 September 2017; published 29 November 2017)

The pseudogap metal phase of the hole-doped cuprate superconductors has two seemingly unrelated characteristics: a gap in the electronic spectrum in the "antinodal" region of the square lattice Brillouin zone and discrete broken symmetries. We present a SU(2) gauge theory of quantum fluctuations of magnetically ordered states which appear in a classical theory of square lattice antiferromagnets, in a spin-density wave mean field theory of the square lattice Hubbard model, and in a $\mathbb{CP}^1$ theory of spinons. This theory leads to metals with an antinodal gap and topological order which intertwines with the observed broken symmetries.

DOI: 10.1103/PhysRevLett.119.227002

A remarkable property of the pseudogap metal of the hole-doped cuprates is that it does not exhibit a "large" Fermi surface of gapless electronlike quasiparticles excitations; i.e., the size of the Fermi surface is smaller than expected from the classic Luttinger theorem of Fermi liquid theory [1]. Instead, it has a gap in the fermionic spectrum near the "antinodal" points $[(\pi, 0)$ and $(0, \pi)]$ of the square lattice Brillouin zone. Gapless fermionic excitations appear to be present only along the diagonals of the Brillouin zone (the "nodal" region). One way to obtain such a Fermi surface reconstruction is by a broken translational symmetry. However, there is no sign of broken translational symmetry over a wide intermediate temperature range [2], and also at low temperatures and intermediate doping [3], over which the pseudogap is present. With full translational symmetry, violations of the Luttinger theorem require the presence of topological order [4–6].

A seemingly unrelated property of the pseudogap metal is that it exhibits discrete broken symmetries, which preserve translations, over roughly the same region of the phase diagram over which there is an antinodal gap in the fermionic spectrum. The broken symmetries include lattice rotations, interpreted in terms of an Ising-nematic order [7–10], and one or both of inversion and time-reversal symmetry breaking [11–16]. Luttinger's theorem implies that none of these broken symmetries can induce the needed fermionic gap by themselves.

The coexistence of the antinodal gap and the broken symmetries can be explained by intertwining them [17–19], i.e., by exploiting flavors of topological order which are tied to specific broken symmetries. Here we show that broken lattice rotations, inversion, and time reversal appear naturally in several models appropriate to the known cuprate electronic structure.

We consider quantum fluctuations of magnetically ordered states found in two different computations: a classical theory of frustrated, insulating antiferromagnets on the square lattice and a spin-density wave theory of metallic states of the square lattice Hubbard model. The types of magnetically ordered states found are sketched in Fig. 1(a). The quantum fluctuations of these states are described by a SU(2) gauge theory, and this leads to the loss of magnetic order and the appearance of phases with topological order and an antinodal gap in the fermion spectrum. We find that the topological order intertwines with precisely the observed broken discrete symmetries, as shown in Fig. 1(b). We further show that the same phases are also obtained naturally in a $\mathbb{CP}^1$ theory of bosonic spinons supplemented by Higgs fields conjugate to long-wavelength spinon pairs.

Magnetic order.—We examine states in which the electron spin $\hat{\boldsymbol{S}}_i$ on site i of the square lattice, at position $\boldsymbol{r}_i$, has the expectation value

$$\langle \hat{\boldsymbol{S}}_i \rangle = N_0[\cos(\boldsymbol{K}\cdot\boldsymbol{r}_i)\cos(\theta)\hat{\boldsymbol{e}}_x + \sin(\boldsymbol{K}\cdot\boldsymbol{r}_i)\cos(\theta)\hat{\boldsymbol{e}}_y + \sin(\theta)\hat{\boldsymbol{e}}_z]. \quad (1)$$

The different states we find are [see Fig. 1(a)] (D') a Néel state with collinear antiferromagnetism at wave vector (π, π), with $\boldsymbol{K} = (\pi, \pi)$, $\theta = 0$, (A') a canted state, with (π, π) Néel order coexisting with a ferromagnet moment perpendicular to the Néel order, with $\boldsymbol{K} = (\pi, \pi)$, $0 < \theta < \pi/2$, (B') a planar spiral state, in which the spins precess at an incommensurate wave vector $\boldsymbol{K}$ with $\theta = 0$, and (C') a conical spiral state, which is a planar spiral accompanied by a ferromagnetic moment perpendicular to the plane of the spiral [20] with $\boldsymbol{K}$ incommensurate, $0 < \theta < \pi/2$.

First, we study the square lattice spin Hamiltonian with near-neighbor antiferromagnetic exchange interactions $J_p > 0$ and ring exchange K [21–25]:

$$\mathcal{H}_J = \sum_{i<j} J_{ij}\hat{\boldsymbol{S}}_i\cdot\hat{\boldsymbol{S}}_j + 2K\sum_{\substack{k \\ j\square i}}^{\ell}[(\hat{\boldsymbol{S}}_i\cdot\hat{\boldsymbol{S}}_j)(\hat{\boldsymbol{S}}_k\cdot\hat{\boldsymbol{S}}_\ell) + (\hat{\boldsymbol{S}}_i\cdot\hat{\boldsymbol{S}}_\ell)(\hat{\boldsymbol{S}}_k\cdot\hat{\boldsymbol{S}}_j) - (\hat{\boldsymbol{S}}_i\cdot\hat{\boldsymbol{S}}_k)(\hat{\boldsymbol{S}}_j\cdot\hat{\boldsymbol{S}}_\ell)]. \quad (2)$$

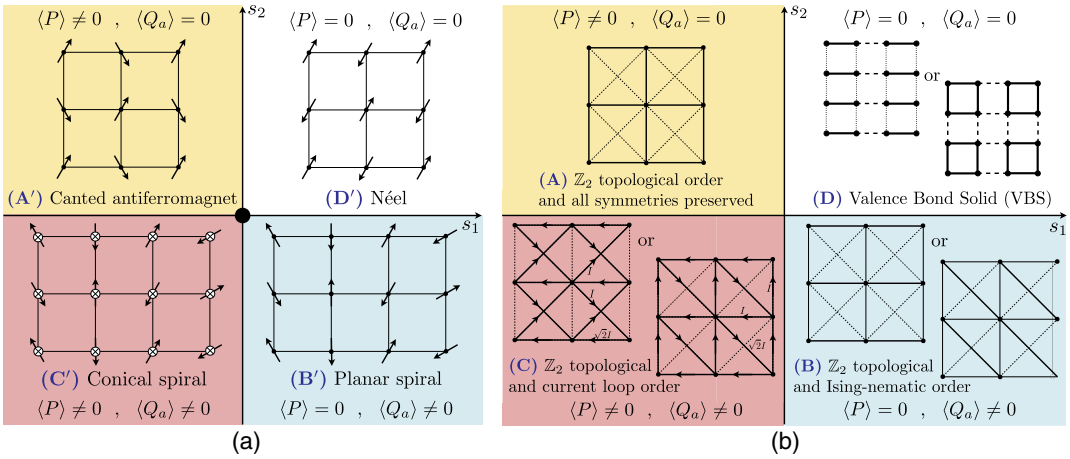

FIG. 1. (a) Schematics of the magnetically ordered states obtained in the classical antiferromagnet and in the spin-density wave theory of the Hubbard model. (b) Corresponding states obtained after quantum fluctuations restore spin rotation symmetry. Phase D has U(1) topological order in the metal but is unstable to the appearance of VBS order in the insulator. The crossed circles in phase C' indicate a canting of the spins into the plane. The labels s_1, s_2, P, and Q_a refer to the $\mathbb{CP}^1$ theory: The phases in (a) are obtained for small g, and those in (b) for large g.

$J_{ij} = J_p$ when i and j are pth nearest neighbors, and we allow J_p only with $p = 1, 2, 3, 4$ nonzero. The classical ground states are obtained by minimizing $\mathcal{H}_J$ over the set of states in Eq. (1); results are shown in Figs. 2(a)–2(c). We find the states A', B', C', and D', all of which meet at a multicritical point, just as in the schematic phase diagram in Fig. 1(a). A semiclassical theory of quantum fluctuations about these states, starting from the Néel state, appears in Supplemental Material Sec. A [26].

For metallic states with spin-density wave order [32–35], we study the Hubbard model

$$\mathcal{H}_U = -\sum_{i<j,\alpha} t_{ij} c^\dagger_{i,\alpha} c_{j,\alpha} - \mu \sum_{i,\alpha} c^\dagger_{i,\alpha} c_{i,\alpha} + U \sum_i \hat{n}_{i,\uparrow} \hat{n}_{i,\downarrow} \qquad (3)$$

of electrons $c_{i,\alpha}$, with $\alpha = \uparrow, \downarrow$ a spin index, $t_{ij} = t_p$ when i and j are pth nearest neighbors, and we take t_p with $p = 1$, 2, 3, 4 nonzero. U is the on-site Coulomb repulsion, and μ is the chemical potential. The electron density $\hat{n}_{i,\alpha} \equiv c^\dagger_{i,\alpha} c_{i,\alpha}$, while the electron spin $\hat{\mathbf{S}}_i \equiv (1/2) c^\dagger_{i,\alpha} \boldsymbol{\sigma}_{\alpha\beta} c_{i,\beta}$, with $\boldsymbol{\sigma}$ the Pauli matrices. We minimized $\mathcal{H}_U$ over the set of free fermion Slater determinant states obeying Eq. (1) while maintaining uniform charge and current densities; Results are illustrated in Figs. 2(d)–2(f), and details appear in Supplemental Material Sec. B [26]. Again, note the appearance of the magnetic orders A', B', C', and D', although now these coexist with Fermi surfaces and metallic conduction.

SU(2) gauge theory.—We describe quantum fluctuations about states of $\mathcal{H}_U$ obeying Eq. (1) by transforming the

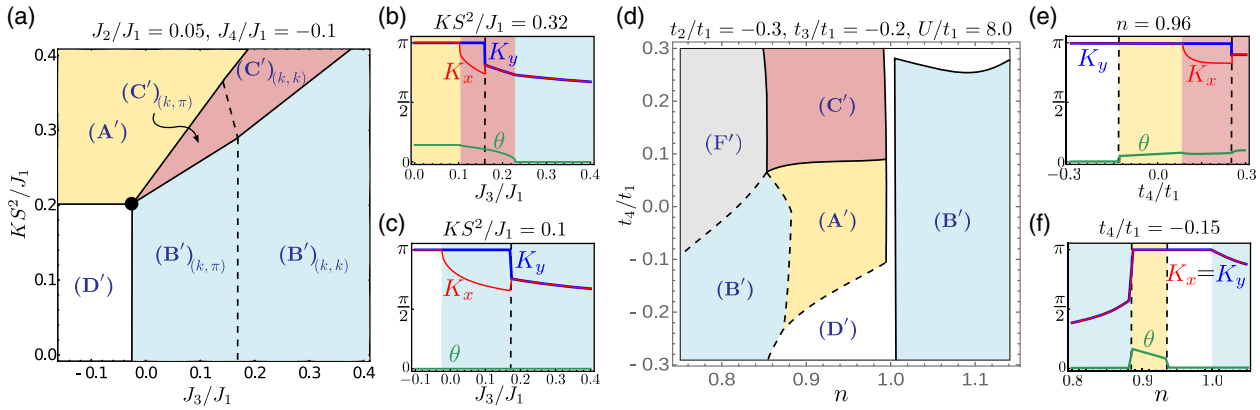

FIG. 2. (a) Phase diagram of $\mathcal{H}_J$, for a spin S model in the classical limit $S \to \infty$, exhibiting all phases of Fig. 1(a). The subscript of the labels (B') and (C') indicates the wave vector $\boldsymbol{K} = (K_x, K_y)$ of the spiral. Note that the phases A', C', B', and D' meet at a multicritical point, just as in Fig. 1(a). (b) and (c) show K_x, K_y, and the canting angle θ along two different one-dimensional cuts of the phase diagram in (a). The phase diagram resulting from the spin-density wave analysis of the Hubbard model (3) can be found in (d). Besides an additional ferromagnetic phase, denoted by (F'), we recover all the phases of the classical phase diagram in (a). Parts (e) and (f) show one-dimensional cuts of the spin-density wave phase diagram. In all figures, solid (dashed) lines are used to represent second- (first-) order transitions.

electrons to a rotating reference frame by a SU(2) matrix R_i [36]:

$$\begin{pmatrix} c_{i,\uparrow} \\ c_{i,\downarrow} \end{pmatrix} = R_i \begin{pmatrix} \psi_{i,+} \\ \psi_{i,-} \end{pmatrix}, \qquad R_i^\dagger R_i = R_i R_i^\dagger = \mathbb{1}. \quad (4)$$

The fermions in the rotating reference frame are spinless "chargons" ψ_s, with $s = \pm$, carrying the electromagnetic charge. In the same manner, the transformation of the electron spin operator $\hat{\boldsymbol{S}}_i$ to the rotating reference frame is proportional to the "Higgs" field $\boldsymbol{H}_i$ [36]:

$$\boldsymbol{\sigma} \cdot \boldsymbol{H}_i \propto R_i^\dagger \boldsymbol{\sigma} \cdot \hat{\boldsymbol{S}}_i R_i. \quad (5)$$

The new variables ψ, R, and $\boldsymbol{H}$ provide a formally redundant description of the physics of $\mathcal{H}_U$, as all observables are invariant under a SU(2) gauge transformation V_i under which

$$\begin{aligned} R_i &\to R_i V_i^\dagger \\ \boldsymbol{\sigma} \cdot \boldsymbol{H}_i &\to V_i \boldsymbol{\sigma} \cdot \boldsymbol{H}_i V_i^\dagger \end{aligned} \begin{pmatrix} \psi_{i,+} \\ \psi_{i,-} \end{pmatrix} \to V_i \begin{pmatrix} \psi_{i,+} \\ \psi_{i,-} \end{pmatrix}, \quad (6)$$

while c_i and $\hat{\boldsymbol{S}}_i$ are gauge invariant. The action of the SU(2) gauge transformation V_i should be distinguished from the action of global SU(2) spin rotations Ω under which

$$\begin{aligned} R_i &\to \Omega R_i \\ \boldsymbol{\sigma} \cdot \hat{\boldsymbol{S}}_i &\to \Omega \boldsymbol{\sigma} \cdot \hat{\boldsymbol{S}}_i \Omega^\dagger \end{aligned} \begin{pmatrix} c_{i\uparrow} \\ c_{i\downarrow} \end{pmatrix} \to \Omega \begin{pmatrix} c_{i\uparrow} \\ c_{i\downarrow} \end{pmatrix}, \quad (7)$$

while ψ and $\boldsymbol{H}$ are invariant.

In the language of this SU(2) gauge theory [36,37], the phases with magnetic order obtained above appear when both R and $\boldsymbol{H}$ are condensed. We may choose a gauge in which $\langle R \rangle \propto \mathbb{1}$, and so the orientation of the $\boldsymbol{H}$ condensate is the same as that in Eq. (1):

$$\langle \boldsymbol{H}_i \rangle = H_0 \Big[\cos(\boldsymbol{K} \cdot \boldsymbol{r}_i) \cos(\theta) \hat{\boldsymbol{e}}_x + \sin(\boldsymbol{K} \cdot \boldsymbol{r}_i) \cos(\theta) \hat{\boldsymbol{e}}_y + \sin(\theta) \hat{\boldsymbol{e}}_z \Big]. \quad (8)$$

We can now obtain the phases of $\mathcal{H}_U$ with quantum fluctuating spin-density wave order, (A, B, C, D) shown in Fig. 1(b), in a simple step: The quantum fluctuations lead to fluctuations in the orientation of the local magnetic order and so remove the R condensate leading to $\langle R \rangle = 0$. The Higgs field $\boldsymbol{H}_i$ retains the condensate in Eq. (8), indicating that the magnitude of the local order is nonzero. In such a phase, spin rotation invariance is maintained with $\langle \hat{\boldsymbol{S}} \rangle = 0$, but the SU(2) gauge group has been "Higgsed" down to a smaller gauge group which describes the topological order [17,38–42]. The values of θ and $\boldsymbol{K}$ in phases (A, B, C, D) obey the same constraints as the corresponding magnetically ordered phases (A', B', C', D'). In phase D, the gauge group is broken down to U(1), and there is a potentially gapless emergent "photon"; in an insulator, monopole condensation drives confinement and the appearance of valence bond solid (VBS) order, but the photon survives in a metallic, U(1) "algebraic charge liquid" (ACL) state [43] (which is eventually unstable to fermion pairing and superconductivity [44]). The remaining phases A, B, and C have a noncollinear configuration of $\langle \boldsymbol{H}_i \rangle$, and then only $\mathbb{Z}_2$ topological order survives [17]: Such states are ACLs with stable, gapped, "vison" excitations carrying $\mathbb{Z}_2$ gauge flux which cannot be created singly by any local operator. Phase A breaks no symmetries, phase B breaks lattice rotation symmetry leading to Ising-nematic order [17,38], and phase C has broken time-reversal and mirror symmetries (but not their product), leading to current loop order [45]. All four ACL phases (A, B, C, D) may also become "fractionalized Fermi liquids" (FL*) [4,5] by the formation of bound states between the chargons and R; the FL* states have a Pauli contribution to the spin susceptibility from the reconstructed Fermi surfaces.

The structure of the fermionic excitations in the phases of Fig. 1(b), and the possible broken symmetries in the $\mathbb{Z}_2$ phases, can be understood from an effective Hamiltonian for the chargons. As described in Supplemental Material Sec. C [26], a Hubbard-Stratonovich transformation on $\mathcal{H}_U$, followed by the change of variables in Eqs. (4) and (5), and a mean field decoupling leads to

$$\mathcal{H}_\psi = -\sum_{i<j,s} t_{ij} Z_{ij} \psi_{i,s}^\dagger \psi_{j,s} - \mu \sum_{i,s} \psi_{i,s}^\dagger \psi_{i,s} - \sum_{i,s,s'} \boldsymbol{H}_i \cdot \psi_{i,s}^\dagger \boldsymbol{\sigma}_{ss'} \psi_{i,s'}. \quad (9)$$

The chargons inherit their hopping from the electrons, apart from a renormalization factor Z_{ij}, and experience a Zeeman-like coupling to a local field given by the condensate of $\boldsymbol{H}$: So the Fermi surface of ψ reconstructs in the same manner as the Fermi surface of c in the phases with conventional spin-density wave order. Note that this happens here even though translational symmetry is fully preserved in all gauge-invariant observables; the apparent breaking of translational symmetry in the Higgs condensate in Eq. (8) does not transfer to any gauge-invariant observables, showing how the Luttinger theorem can be violated by the topological order [4–6] in Higgs phases. However, other symmetries are broken in gauge-invariant observables: Supplemental Material Sec. C [26] examines bond and current variables, which are bilinears in ψ, and finds that they break symmetries in phases B and C noted above.

$\mathbb{CP}^1$ theory.—We now present an alternative description of all eight phases in Fig. 1 starting from the popular $\mathbb{CP}^1$ theory of quantum antiferromagnets. In principle (as we note below and in Supplemental Material Sec. D [26]), this theory can be derived from the SU(2) gauge theory above [46] after integrating out the fermionic chargons and representing R in terms of a bosonic spinon field z_α by

$$R_i = \begin{pmatrix} z_{i,\uparrow} & -z_{i,\downarrow}^* \\ z_{i,\downarrow} & z_{i,\uparrow}^* \end{pmatrix}, \qquad |z_{i,\uparrow}|^2 + |z_{i,\downarrow}|^2 = 1. \quad (10)$$

However, integrating out the chargons is safe only when there is a chargon gap, and so the theories below can compute critical properties of phase transitions only in insulators.

We will not start here from the SU(2) gauge theory but present a direct derivation from earlier analyses of the quantum fluctuations of an $S = 1/2$ square lattice antiferromagnet near a Néel state, which obtained the following action [47] for a $\mathbb{CP}^1$ theory over two-dimensional space $[r = (x, y)]$ and time (t):

$$\mathcal{S} = \frac{1}{g}\int d^2 r dt |(\partial_\mu - i a_\mu) z_\alpha|^2 + \mathcal{S}_B. \tag{11}$$

Here μ runs over three spacetime components, and a_μ is an emergent U(1) gauge field. The local Néel order $\boldsymbol{n}$ is related to the z_α by $\boldsymbol{n} = z_\alpha^* \boldsymbol{\sigma}_{\alpha\beta} z_\beta$, where $\boldsymbol{\sigma}$ are the Pauli matrices. The U(1) gauge flux is defined modulo 2π, and so the gauge field is compact and monopole configurations with total flux 2π are permitted in the path integral. The continuum action in Eq. (11) should be regularized to allow such monopoles. $\mathcal{S}_B$ is the Berry phase of the monopoles [48–50]. Monopoles are suppressed in the states with $\mathbb{Z}_2$ topological order [17,38], and so we do not display the explicit form of $\mathcal{S}_B$.

The phases of the $\mathbb{CP}^1$ theory in Eq. (11) have been extensively studied. For small g, we have the conventional Néel state, D' in Fig. 1(a), with $\langle z_\alpha \rangle \neq 0$ and $\langle \boldsymbol{n} \rangle \neq 0$. For large g, the z_α are gapped, and the confinement in the compact U(1) gauge theory leads to VBS order [49,50], which is phase D in Fig. 1(b). A deconfined critical theory describes the transition between these phases [51].

We now want to extend the theory in Eq. (11) to avoid confinement and obtain states with topological order. In a compact U(1) gauge theory, condensing a Higgs field with charge 2 leads to a phase with deconfined $\mathbb{Z}_2$ charges [52]. Such a deconfined phase has the $\mathbb{Z}_2$ topological order [17,38–42] of interest to us here. So we search for candidate Higgs fields with charge 2, composed of pairs of long-wavelength spinons, z_α. We also require the Higgs field to be spin rotation invariant, because we want the $\mathbb{Z}_2$ topological order to persist in phases without magnetic order. The simplest candidate without spacetime gradients, $\varepsilon_{\alpha\beta} z_\alpha z_\beta$ (where $\varepsilon_{\alpha\beta}$ is the unit antisymmetric tensor), vanishes identically. Therefore, we are led to the following Higgs candidates with a single gradient $(a = x, y)$:

$$P \sim \varepsilon_{\alpha\beta} z_\alpha \partial_t z_\beta, \qquad Q_a \sim \varepsilon_{\alpha\beta} z_\alpha \partial_a z_\beta. \tag{12}$$

These Higgs fields have been considered separately before. Condensing Q_a was the route to $\mathbb{Z}_2$ topological order in Ref. [38], while P appeared more recently in Ref. [53].

The effective action for these Higgs fields and the properties of the Higgs phases follow straightforwardly from their transformations under the square lattice space group and time reversal: We collect these in Table I.

TABLE I. Symmetry signatures of various fields under time reversal ($\mathcal{T}$), translation by a lattice spacing along x (T_x), reflection about a lattice site with $x \to -x$, $y \to y$ (I_x), and rotation by $\pi/2$ about a lattice site with $x \to y$, $y \to -x$ ($R_{\pi/2}$).

	$\mathcal{T}$	T_x	I_x	$R_{\pi/2}$
z_α	$\varepsilon_{\alpha\beta} z_\beta$	$\varepsilon_{\alpha\beta} z_\beta^*$	z_α	z_α
Q_x	Q_x	Q_x^*	$-Q_x$	Q_y
Q_y	Q_y	Q_y^*	Q_y	$-Q_x$
P	$-P$	P^*	P	P

From these transformations, we can add to the action $\mathcal{S} \to \mathcal{S} + \int d^2 r dt \mathcal{L}_{P,Q}$:

$$\begin{aligned}\mathcal{L}_{P,Q} = {} & |(\partial_\mu - 2 i a_\mu) P|^2 + |(\partial_\mu - 2 i a_\mu) Q_a|^2 \\ & + \lambda_1 P^* \varepsilon_{\alpha\beta} z_\alpha \partial_t z_\beta + \lambda_2 Q_a^* \varepsilon_{\alpha\beta} z_\alpha \partial_a z_\beta + \text{H.c.} \\ & - s_1 |P|^2 - s_2 |Q_a|^2 - u_1 |P|^4 - u_2 |Q_a|^4 + \cdots,\end{aligned} \tag{13}$$

where we do not display other quartic and higher-order terms in the Higgs potential.

For large g, we have $\langle z_\alpha \rangle = 0$ and can then determine the spin liquid phases by minimizing the Higgs potential as a function of s_1 and s_2. When there is no Higgs condensate, we noted earlier that we obtain phase D in Fig. 1(b). Figure 1(b) also indicates that the phases A, B, and C are obtained when one or both of the P and Q_a condensates are present. This is justified in Supplemental Material Sec. D [26] by a computation of the quadratic effective action for the z_α from the SU(2) gauge theory: We find just the terms with linear temporal and/or spatial derivatives as would be expected from the presence of P and/or Q_a condensates in $\mathcal{L}_{P,Q}$.

We can confirm this identification from the symmetry transformations in Table I: (A) There is only a P condensate, and the gauge-invariant quantity $|P|^2$ is invariant under all symmetry operations. Consequently, this is a $\mathbb{Z}_2$ spin liquid with no broken symmetries; it has been previously studied by Yang and Wang [53] using bosonic spinons. (B) With a Q_a condensate, one of the two gauge-invariant quantities $|Q_x|^2 - |Q_y|^2$ or $Q_x^* Q_y + Q_x Q_y^*$ must have a nonzero expectation value. Table I shows that these imply Ising-nematic order, as described previously [17,38,54]. We also require $\langle Q_x \rangle \langle Q_y^* \rangle$ to be real to avoid breaking translational symmetry. (C) With both and P and Q_a condensates nonzero, we can define the gauge-invariant order parameter $O_a = P Q_a^* + P^* Q_a$ (again, $\langle P \rangle \langle Q_a^* \rangle$ should be real to avoid translational symmetry breaking). The symmetry transformations of O_a show that it is precisely the "current-loop" order parameter of Ref. [19]: It is odd under reflection and time reversal but not their product.

A similar analysis can be carried out at small g, where z_α condenses and breaks spin rotation symmetry. The structure of the condensate is determined by the eigenmodes of the z_α dispersion in the A, B, C, D phases, and this determines

that the corresponding magnetically ordered states are precisely A', B', C', D', as in Fig. 1(a).

We have shown here that a class of topological orders intertwine with the observed broken discrete symmetries in the pseudogap phase of the hole-doped cuprates. The same topological orders emerge from a theory of quantum fluctuations of magnetically ordered states obtained by four different methods: the frustrated classical antiferromagnet, the semiclassical nonlinear sigma model, the spin-density wave theory, and the $\mathbb{CP}^1$ theory supplemented by the Higgs fields obtained by pairing spinons at long wavelengths. The intertwining of topological order and symmetries can explain why the symmetries are restored when the pseudogap in the fermion spectrum disappears at large doping.

We thank A. Chubukov, A. Eberlein, D. Hsieh, Yin-Chen He, B. Keimer, T. V. Raziman, T. Senthil, and A. Thomson for useful discussions. This research was supported by the NSF under Grant No. DMR-1664842 and the MURI Grant No. W911NF-14-1-0003 from ARO. Research at Perimeter Institute is supported by the Government of Canada through Industry Canada and by the Province of Ontario through the Ministry of Research and Innovation. S. S. also acknowledges support from Cenovus Energy at Perimeter Institute. M. S. S. acknowledges support from the German National Academy of Sciences Leopoldina through Grant No. LPDS 2016-12.

[1] J. M. Luttinger and J. C. Ward, Ground-State energy of a many-fermion system. II, Phys. Rev. **118**, 1417 (1960).
[2] B. Keimer, S. A. Kivelson, M. R. Norman, S. Uchida, and J. Zaanen, From quantum matter to high-temperature superconductivity in copper oxides, Nature (London) **518**, 179 (2015).
[3] S. Badoux, W. Tabis, F. Laliberté, G. Grissonnanche, B. Vignolle, D. Vignolles, J. Béard, D. A. Bonn, W. N. Hardy, R. Liang, N. Doiron-Leyraud, L. Taillefer, and C. Proust, Change of carrier density at the pseudogap critical point of a cuprate superconductor, Nature (London) **531**, 210 (2016).
[4] T. Senthil, S. Sachdev, and M. Vojta, Fractionalized Fermi Liquids, Phys. Rev. Lett. **90**, 216403 (2003).
[5] T. Senthil, M. Vojta, and S. Sachdev, Weak magnetism and non-Fermi liquids near heavy-fermion critical points, Phys. Rev. B **69**, 035111 (2004).
[6] A. Paramekanti and A. Vishwanath, Extending Luttinger's theorem to $\mathbb{Z}_2$ fractionalized phases of matter, Phys. Rev. B **70**, 245118 (2004).
[7] Y. Ando, K. Segawa, S. Komiya, and A. N. Lavrov, Electrical Resistivity Anisotropy from Self-Organized One Dimensionality in High-Temperature Superconductors, Phys. Rev. Lett. **88**, 137005 (2002).
[8] V. Hinkov, D. Haug, B. Fauqué, P. Bourges, Y. Sidis, A. Ivanov, C. Bernhard, C. T. Lin, and B. Keimer, Electronic liquid crystal state in the high-temperature superconductor $YBa_2Cu_3O_{6.45}$, Science **319**, 597 (2008).
[9] R. Daou, J. Chang, D. Leboeuf, O. Cyr-Choinière, F. Laliberté, N. Doiron-Leyraud, B. J. Ramshaw, R. Liang, D. A. Bonn, W. N. Hardy, and L. Taillefer, Broken rotational symmetry in the pseudogap phase of a high-T_c superconductor, Nature (London) **463**, 519 (2010).
[10] M. J. Lawler, K. Fujita, J. Lee, A. R. Schmidt, Y. Kohsaka, C. K. Kim, H. Eisaki, S. Uchida, J. C. Davis, J. P. Sethna, and E.-A. Kim, Intra-unit-cell electronic nematicity of the high-T_c copper-oxide pseudogap states, Nature (London) **466**, 347 (2010).
[11] J. Xia, E. Schemm, G. Deutscher, S. A. Kivelson, D. A. Bonn, W. N. Hardy, R. Liang, W. Siemons, G. Koster, M. M. Fejer, and A. Kapitulnik, Polar Kerr-Effect Measurements of the High-Temperature $YBa_2Cu_3O_{6+x}$ Superconductor: Evidence for Broken Symmetry near the Pseudogap Temperature, Phys. Rev. Lett. **100**, 127002 (2008).
[12] Y. Lubashevsky, L. D. Pan, T. Kirzhner, G. Koren, and N. P. Armitage, Optical Birefringence and Dichroism of Cuprate Superconductors in the THz Regime, Phys. Rev. Lett. **112**, 147001 (2014).
[13] L. Mangin-Thro, Y. Sidis, A. Wildes, and P. Bourges, Intra-unit-cell magnetic correlations near optimal doping in $YBa_2Cu_3O_{6.85}$, Nat. Commun. **6**, 7705 (2015).
[14] L. Zhao, C. A. Belvin, R. Liang, D. A. Bonn, W. N. Hardy, N. P. Armitage, and D. Hsieh, A global inversion-symmetry-broken phase inside the pseudogap region of $YBa_2Cu_3O_y$, Nat. Phys. **13**, 250 (2017).
[15] A. Pal, S. R. Dunsiger, K. Akintola, A. C. Y. Fang, A. Elhosary, M. Ishikado, H. Eisaki, and J. E. Sonier, Quasi-static internal magnetic field detected in the pseudogap phase of $Bi_{2+x}Sr_{2-x}CaCu_2O_{8+\delta}$ by μSR, arXiv:1707.01111.
[16] T. P. Croft, E. Blackburn, J. Kulda, R. Liang, D. A. Bonn, W. N. Hardy, and S. M. Hayden, No evidence for orbital loop currents in charge ordered $YBa_2Cu_3O_{6+x}$ from polarized neutron diffraction, arXiv:1709.06128.
[17] S. Sachdev and N. Read, Large N expansion for frustrated and doped quantum antiferromagnets, Int. J. Mod. Phys. B **05**, 219 (1991).
[18] M. Barkeshli, H. Yao, and S. A. Kivelson, Gapless spin liquids: Stability and possible experimental relevance, Phys. Rev. B **87**, 140402 (2013).
[19] S. Chatterjee and S. Sachdev, Insulators and metals with topological order and discrete symmetry breaking, Phys. Rev. B **95**, 205133 (2017).
[20] Y. Yoshida, S. Schröder, P. Ferriani, D. Serrate, A. Kubetzka, K. von Bergmann, S. Heinze, and R. Wiesendanger, Conical Spin-Spiral State in an Ultrathin Film Driven by Higher-Order Spin Interactions, Phys. Rev. Lett. **108**, 087205 (2012).
[21] A. H. MacDonald, S. M. Girvin, and D. Yoshioka, t/U expansion for the Hubbard model, Phys. Rev. B **37**, 9753 (1988).
[22] R. R. P. Singh, M. P. Gelfand, and D. A. Huse, Ground States of Low-Dimensional Quantum Antiferromagnets, Phys. Rev. Lett. **61**, 2484 (1988).
[23] A. Chubukov, E. Gagliano, and C. Balseiro, Phase diagram of the frustrated spin-1/2 Heisenberg antiferromagnet with cyclic-exchange interaction, Phys. Rev. B **45**, 7889 (1992).
[24] A. Läuchli, J. C. Domenge, C. Lhuillier, P. Sindzingre, and M. Troyer, Two-Step Restoration of SU(2) Symmetry in a

Frustrated Ring-Exchange Magnet, Phys. Rev. Lett. **95**, 137206 (2005).
[25] K. Majumdar, D. Furton, and G. S. Uhrig, Effects of ring exchange interaction on the Néel phase of two-dimensional, spatially anisotropic, frustrated Heisenberg quantum antiferromagnet, Phys. Rev. B **85**, 144420 (2012).
[26] See Supplemental Material at http://link.aps.org/supplemental/10.1103/PhysRevLett.119.227002 for the discussion of the semiclassical sigma model, more details on the spin-wave-theory analysis of the Hubbard model, the derivation and symmetries of the effective chargon Hamiltonian, and the derivation of the $\mathbb{CP}^1$ theory from the SU(2) gauge theory, which includes Refs. [27–31].
[27] S. Sachdev, *Quantum Phase Transitions*, 2nd ed. (Cambridge University Press, Cambridge, United Kingdom, 2011).
[28] J. G. Storey, Hall effect and Fermi surface reconstruction via electron pockets in the high-T_c cuprates, Europhys. Lett. **113**, 27003 (2016).
[29] A. Eberlein, W. Metzner, S. Sachdev, and H. Yamase, Fermi Surface Reconstruction and Drop in the Hall Number due to Spiral Antiferromagnetism in High-T_c Cuprates, Phys. Rev. Lett. **117**, 187001 (2016).
[30] S. Chatterjee, S. Sachdev, and A. Eberlein, Thermal and electrical transport in metals and superconductors across antiferromagnetic and topological quantum transitions, Phys. Rev. B **96**, 075103 (2017).
[31] M. Charlebois, S. Verret, A. Foley, O. Simard, D. Sénéchal, and A. Tremblay, Hall effect in cuprates with incommensurate spin-density wave, Phys. Rev. B **96**, 205132 (2017).
[32] M. Inui and P. B. Littlewood, Hartree-Fock study of the magnetism in the single-band Hubbard model, Phys. Rev. B **44**, 4415 (1991).
[33] E. Arrigoni and G. C. Strinati, Doping-induced incommensurate antiferromagnetism in a Mott-Hubbard insulator, Phys. Rev. B **44**, 7455 (1991).
[34] M. Dzierzawa, Hartree-Fock theory of spiral magnetic order in the 2-*d* Hubbard model, Z. Phys. B **86**, 49 (1992).
[35] P. A. Igoshev, M. A. Timirgazin, A. A. Katanin, A. K. Arzhnikov, and V. Y. Irkhin, Incommensurate magnetic order and phase separation in the two-dimensional Hubbard model with nearest- and next-nearest-neighbor hopping, Phys. Rev. B **81**, 094407 (2010).
[36] S. Sachdev, M. A. Metlitski, Y. Qi, and C. Xu, Fluctuating spin density waves in metals, Phys. Rev. B **80**, 155129 (2009).
[37] D. Chowdhury and S. Sachdev, Higgs criticality in a two-dimensional metal, Phys. Rev. B **91**, 115123 (2015).
[38] N. Read and S. Sachdev, Large N Expansion for Frustrated Quantum Antiferromagnets, Phys. Rev. Lett. **66**, 1773 (1991).
[39] X. G. Wen, Mean-field theory of spin-liquid states with finite energy gap and topological orders, Phys. Rev. B **44**, 2664 (1991).
[40] F. A. Bais, P. van Driel, and M. de Wild Propitius, Quantum symmetries in discrete gauge theories, Phys. Lett. B **280**, 63 (1992).
[41] J. M. Maldacena, G. W. Moore, and N. Seiberg, D-brane charges in five-brane backgrounds, J. High Energy Phys. 10 (2001) 005.
[42] T. H. Hansson, V. Oganesyan, and S. L. Sondhi, Superconductors are topologically ordered, Ann. Phys. (Amsterdam) **313**, 497 (2004).
[43] R. K. Kaul, Y. B. Kim, S. Sachdev, and T. Senthil, Algebraic charge liquids, Nat. Phys. **4**, 28 (2008).
[44] M. A. Metlitski, D. F. Mross, S. Sachdev, and T. Senthil, Cooper pairing in non-Fermi liquids, Phys. Rev. B **91**, 115111 (2015).
[45] M. E. Simon and C. M. Varma, Detection and Implications of a Time-Reversal Breaking State in Underdoped Cuprates, Phys. Rev. Lett. **89**, 247003 (2002).
[46] M. S. Scheurer, S. Chatterjee, M. Ferrero, A. Georges, S. Sachdev, and W. Wu (unpublished).
[47] S. Sachdev and R. Jalabert, Effective lattice models for two dimensional quantum antiferromagnets, Mod. Phys. Lett. B **04**, 1043 (1990).
[48] F. D. M. Haldane, O(3) Nonlinear σ Model and the Topological Distinction between Integer- and Half-Integer-Spin Antiferromagnets in Two Dimensions, Phys. Rev. Lett. **61**, 1029 (1988).
[49] N. Read and S. Sachdev, Valence-Bond and Spin-Peierls Ground States of Low-Dimensional Quantum Antiferromagnets, Phys. Rev. Lett. **62**, 1694 (1989).
[50] N. Read and S. Sachdev, Spin-Peierls, valence-bond solid, and Néel ground states of low-dimensional quantum antiferromagnets, Phys. Rev. B **42**, 4568 (1990).
[51] T. Senthil, A. Vishwanath, L. Balents, S. Sachdev, and M. P. A. Fisher, Deconfined quantum critical points, Science **303**, 1490 (2004).
[52] E. Fradkin and S. H. Shenker, Phase diagrams of lattice gauge theories with Higgs fields, Phys. Rev. D **19**, 3682 (1979).
[53] X. Yang and F. Wang, Schwinger boson spin-liquid states on square lattice, Phys. Rev. B **94**, 035160 (2016).
[54] S. Chatterjee, Y. Qi, S. Sachdev, and J. Steinberg, Superconductivity from a confinement transition out of a fractionalized Fermi liquid with $\mathbb{Z}_2$ topological and Ising-nematic orders, Phys. Rev. B **94**, 024502 (2016).